

Abnormal magnetic ordering and ferromagnetism in perovskite ScMnO₃ film

F. Wang, Y. Q. Zhang, W. Liu, X. K. Ning, Y. Bai, Z. M. Dai, S. Ma, X. G. Zhao, S. K. Li, and Z. D. Zhang

Citation: [Applied Physics Letters](#) **106**, 232906 (2015); doi: 10.1063/1.4922727

View online: <http://dx.doi.org/10.1063/1.4922727>

View Table of Contents: <http://scitation.aip.org/content/aip/journal/apl/106/23?ver=pdfcov>

Published by the [AIP Publishing](#)

Articles you may be interested in

[Temperature control of local magnetic anisotropy in multiferroic CoFe/BaTiO₃](#)

Appl. Phys. Lett. **102**, 112406 (2013); 10.1063/1.4795529

[Room temperature multiferroic properties of Nd : BiFeO₃ / Bi₂FeMnO₆ bilayered films](#)

Appl. Phys. Lett. **95**, 232904 (2009); 10.1063/1.3271032

[Structural, magnetic, and ferroelectric properties of multiferroic Bi Fe O₃ -based composite films with exchange bias](#)

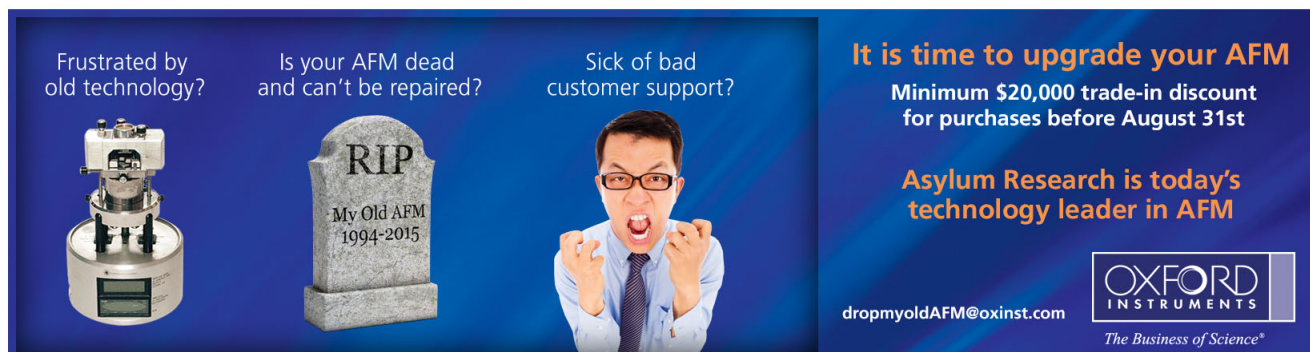
J. Appl. Phys. **105**, 07D903 (2009); 10.1063/1.3055284

[Synthesis and characterization of an n = 6 Aurivillius phase incorporating magnetically active manganese, Bi₇\(Mn, Ti\)₆O₂₁](#)

Appl. Phys. Lett. **91**, 033113 (2007); 10.1063/1.2756163

[Antiferroelectricity in multiferroic Bi Cr O₃ epitaxial films](#)

Appl. Phys. Lett. **89**, 162904 (2006); 10.1063/1.2362585

An advertisement for Oxford Instruments' Asylum Research AFM technology. The background is dark blue. On the left, there is an image of an AFM head. In the center, a man in a suit and glasses looks frustrated, with his hands raised in a 'giving up' gesture. To his right is a tombstone with the inscription 'RIP My Old AFM 1994-2015'. Text on the left asks 'Frustrated by old technology?', 'Is your AFM dead and can't be repaired?', and 'Sick of bad customer support?'. On the right, it says 'It is time to upgrade your AFM' and 'Minimum \$20,000 trade-in discount for purchases before August 31st'. Below that, it states 'Asylum Research is today's technology leader in AFM'. At the bottom right is the Oxford Instruments logo and the tagline 'The Business of Science®'. An email address 'dropmyoldAFM@oxinst.com' is also provided.

Frustrated by old technology?

Is your AFM dead and can't be repaired?

Sick of bad customer support?

It is time to upgrade your AFM

Minimum \$20,000 trade-in discount for purchases before August 31st

Asylum Research is today's technology leader in AFM

dropmyoldAFM@oxinst.com

OXFORD
INSTRUMENTS

The Business of Science®

Abnormal magnetic ordering and ferromagnetism in perovskite ScMnO_3 film

F. Wang, Y. Q. Zhang, W. Liu, X. K. Ning, Y. Bai, Z. M. Dai, S. Ma, X. G. Zhao, S. K. Li, and Z. D. Zhang

Shenyang National Laboratory for Materials Science, Institute of Metal Research, Chinese Academy of Sciences, 72 Wenhua Road, Shenyang 110016, China

(Received 9 April 2015; accepted 6 June 2015; published online 12 June 2015)

Bulk multiferroic ScMnO_3 is the stable hexagonal phase, and it is very difficult to prepare its perovskite orthorhombic phase even under high pressure. We fabricated the orthorhombic ScMnO_3 thin film by pulsed laser deposition through suitable substrate LaAlO_3 and found that nano-scale twin-like domains are naturally formed in the thin film. Magnetic properties of the orthorhombic ScMnO_3 thin films show that, besides normal antiferromagnetic ordering at 47 K, an anomalous magnetic transition occurs at 27 K for 60 nm film and at 36 K for 150 nm film only along the c-axis, which is absent in the ab-plane. Moreover, the second magnetic transition for both films is suppressed when the applied field increases from 1 kOe to 10 kOe. In addition, the ferromagnetism shows up in both films at 10 K, and saturation magnetization increases dramatically in 60 nm film compared with 150 nm film. We propose that the second magnetic transition might be more of lattice strain effect and also related to magnetism-induced ferroelectric polarization in orthorhombic RMnO_3 thin films and low-temperature ferromagnetic properties in our films originate from the nano-scale twin-like domain structure. © 2015 AIP Publishing LLC.

[<http://dx.doi.org/10.1063/1.4922727>]

It is well known that hexagonal RMnO_3 manganites ($R = \text{Ho-Lu, Y, In, and Sc}$) are part of a class of promising multiferroic materials for spintronic application, where an antiferromagnetic transition of Mn^{3+} occurs between 70 K and 130 K, and a ferroelectric transition occurs between 570 K and 990 K due to a structural distortion.^{1,2} The strong coupling between the antiferromagnetic ordering and ferroelectric ordering allows the possibility of controlling magnetism with an electric field (and vice versa).¹⁻⁵ Recently, many researches have been focusing on the metastable orthorhombic phase of RMnO_3 ($R = \text{Ho-Lu, Y, In, and Sc}$) theoretically^{6,7} and experimentally,⁸⁻¹⁵ since the theoretical prediction⁶ that a large spontaneous polarization along a-axis (in $Pbnm$ group symmetry) can be produced in E-type antiferromagnetic orthorhombic RMnO_3 . Since it is very difficult to obtain single-crystal orthorhombic RMnO_3 phase,⁹ most previous studies were performed on polycrystalline samples¹⁰⁻¹⁴ such as polycrystalline orthorhombic RMnO_3 ($R = \text{Ho, Er, Tm, Yb, and Lu}$) fabricated under high pressure or obtained through chemical synthesis.¹⁰⁻¹⁴ However, with R ionic radii (ionic radii for R ions Y^{3+} , Ho^{3+} , Er^{3+} , Tm^{3+} , Yb^{3+} , Lu^{3+} , and Sc^{3+} is 1.02, 1.02, 1.00, 0.99, 0.99, 0.92, and 0.87 Å, respectively) decreasing, the synthesis of polycrystalline orthorhombic RMnO_3 phase also becomes very difficult, especially for smaller R orthorhombic phase such as InMnO_3 and ScMnO_3 .¹⁵⁻¹⁷ Only Tyson's group reported monoclinic ScMnO_3 phase synthesized from the hexagonal phase under 12 GPa and 1100 °C,¹⁵ which exhibits very similar structural parameters to the orthorhombic HoMnO_3 and LuMnO_3 systems. In addition, the difference between the formation energies of the orthorhombic and the hexagonal RMnO_3 phases could be small, so it might be possible to prepare the orthorhombic phase from the hexagonal phase through epitaxial thin-film growth, such as orthorhombic HoMnO_3 thin

film.¹⁸⁻²¹ However, due to contributions from both Mn^{3+} and magnetic Ho^{3+} , the low-temperature magnetic property and the origin of ferroelectric polarization in orthorhombic HoMnO_3 bulk/thin film become more complex. Since Sc^{3+} in ScMnO_3 has no localized magnetic moment, the low-temperature magnetic property becomes relatively simple. Moreover, it was reported recently that nano-scale crystallographic multi-domain structure can induce ferromagnetism in other multiferroic RMnO_3 thin films such as orthorhombic TbMnO_3 and GdMnO_3 films.²²⁻²⁴ In this letter, we fabricated orthorhombic ScMnO_3 thin film grown on LaAlO_3 (001) substrate using a hexagonal target. The crystal structure and magnetic properties are investigated and compared with other orthorhombic RMnO_3 systems.

ScMnO_3 thin films were grown on LaAlO_3 (001) crystal substrate by pulsed laser deposition (PLD) using a KrF ($\lambda = 248$ nm) excimer laser. A hexagonally structured ScMnO_3 target was prepared using solid state sintering. Coherent epitaxial growth, crystal structure, and film orientation of the ScMnO_3 thin film were analyzed by high-resolution transmission electron microscope (HRTEM) and XRD. The crystal structure of both our ScMnO_3 thin film and other introduced bulk/thin films, such as HoMnO_3 and LuMnO_3 , is in $Pbnm$ group symmetry setting in this paper. The surface morphology and ion valence state were characterized by AFM and XPS, respectively, and magnetization measurements were performed from 5 to 300 K using SQUID.

Figures 1(a) and 1(c) show the XRD patterns of 60 nm and 150 nm ScMnO_3 films grown on LaAlO_3 (001) substrate. It is clear that only (002) and (004) reflections of the orthorhombic phase appear along with the substrate peaks in both films, indicating the formation of c-axis oriented pure orthorhombic phase. We also carried out ϕ scans of the in-plane (202) peak of the orthorhombic ScMnO_3 films and the

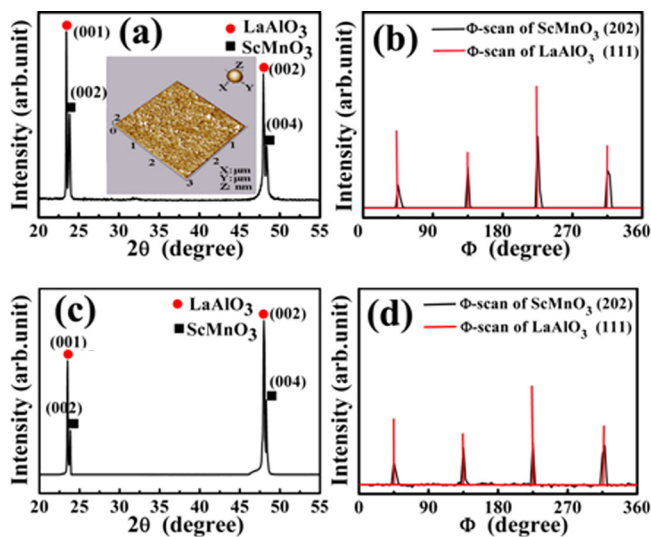


FIG. 1. (a) and (c) θ - 2θ XRD scans of the 60 nm and 150 nm ScMnO₃ films on LaAlO₃ (001) substrate. (b) and (d) ϕ -scans of the in-plane (202) peak of the 60 nm and 150 nm ScMnO₃ films and corresponding (111) peak of LaAlO₃ (001) substrate. The inset of Figure 1(a) is AFM image of 60 nm ScMnO₃ film with $3 \times 3 \mu\text{m}^2$ area.

corresponding (111) peak of LaAlO₃ substrate as shown in Figures 1(b) and 1(d). The ϕ scan shows four symmetric peaks at every 90° rotation angle indicating complete epitaxial growth. This is very similar to the orthorhombic HoMnO₃ film.¹³ Inset of Figure 1(a) shows an AFM image of 60 nm ScMnO₃ film with a $3 \times 3 \mu\text{m}^2$ area. The surface is very smooth with a root mean square (RMS) roughness of 0.69 nm. To further confirm that the ScMnO₃ film is orthorhombic, we carried out HRTEM observation. Figure 2(a)

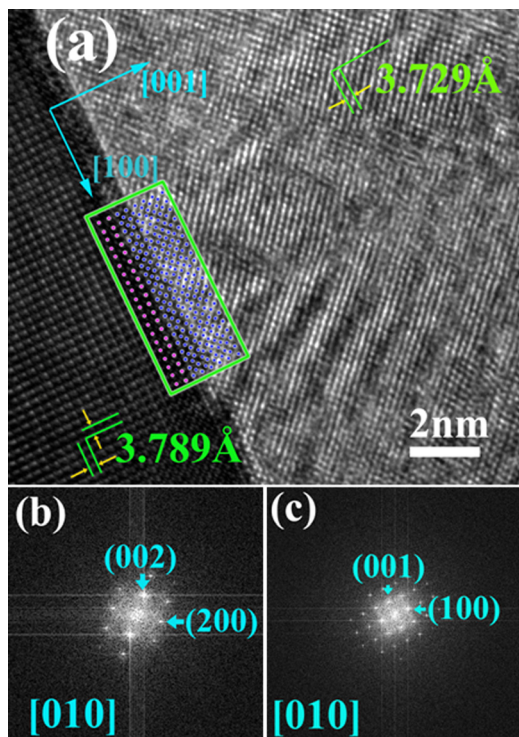


FIG. 2. (a) Cross-section HRTEM image of 60 nm ScMnO₃ film along direction [010] zone axis of substrate LaAlO₃; (b) and (c) fast Fourier transform patterns of the ScMnO₃ film and LaAlO₃ substrate.

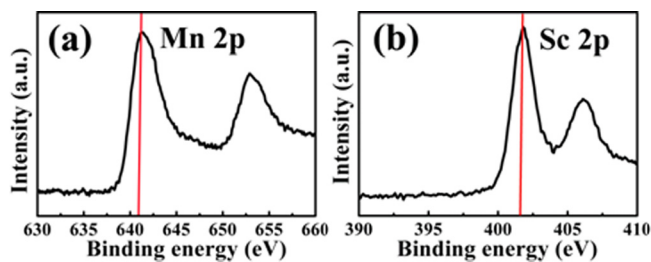


FIG. 3. (a) and (b) the high-resolution narrow-scan XPS spectra of Mn 2p and Sc 2p peaks in 60 nm ScMnO₃ film.

represents the cross-sectional HRTEM image of 60 nm ScMnO₃ film along direction [010] zone axis of substrate LaAlO₃. It can be seen that the ScMnO₃ film grows coherently with the substrate without misfit dislocations along the interface. Figures 2(b) and 2(c) are the fast Fourier transform patterns of the ScMnO₃ film and LaAlO₃ substrate. The (002) and (200) planes of orthorhombic ScMnO₃ phases corresponding to the (001) and (100) planes of substrate LaAlO₃ are observed, further indicating that the crystal structure is orthorhombic.

Figure 3 represents XPS spectra of Mn 2p and Sc 2p peaks in 60 nm ScMnO₃ film. It can be seen from Figures 3(a) and 3(b) that the peaks of Mn 2p_{3/2} and Sc 2p_{3/2} in 60 nm thin film are located at the binding energy of 641.6 eV and 401.9 eV, which correspond to a valence state of Mn³⁺ and Sc³⁺, respectively. It is found from the analysis of the Mn and Sc peaks that the Sc:Mn of the thin film is close to 1:1, indicating that the ScMnO₃ films are stoichiometric, as expected.

Figure 4(a) shows the temperature dependence of magnetization of 60 nm ScMnO₃ thin film along c-axis and in ab-plane at 1 kOe under zero-field-cooled (ZFC) and field-cooled (FC) conditions. Inset of Figure 4(b) is the magnification of low temperature ZFC data from 5 K to 60 K. It is clear that ZFC magnetization data along c axis show two magnetic transitions at 47 K and 27 K, while ZFC magnetization data

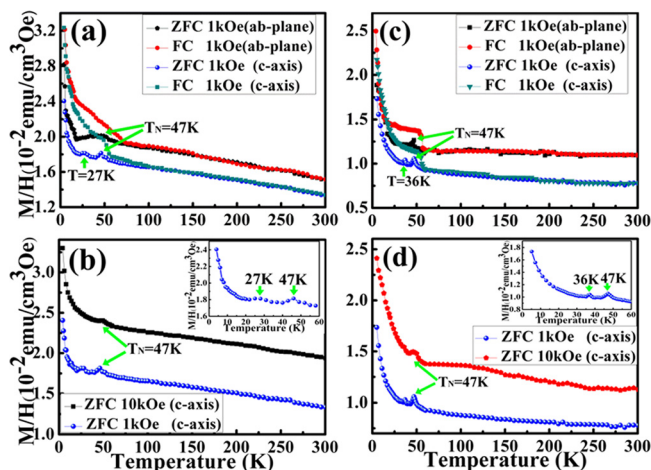


FIG. 4. (a) and (c) ZFC-FC curves measured with a magnetic field of 1 kOe applied along the c-axis and in the ab-plane for 60 nm and 150 nm films, respectively. Figures 4(b) and 4(d) show ZFC curves along the c axis measured at 1 kOe and 10 kOe for 60 nm and 150 nm films, respectively. The insets of Figures 4(b) and 4(d) show enlarged version of the ZFC curve from 5 K to 60 K at 1 kOe for 60 nm and 150 nm films, respectively.

in ab-plane only show one magnetic transition at 47 K. Moreover, the transition at 27 K disappears when a magnetic field of 10 kOe is applied as seen in Figure 4(b). The same as other orthorhombic systems such as HoMnO_3 or LuMnO_3 , magnetic transition at 47 K is the normal antiferromagnetic ordering temperature as expected. In all reported orthorhombic HoMnO_3 and LuMnO_3 films, irrespective of crystal axis direction, the antiferromagnetic ordering temperature is around 40 K and is extremely resistant to lattice strain.^{18–21} Whether the second magnetic transition (or spin reorientation transition of Mn^{3+}) shows up or not and in which crystal direction it appears depend on many factors such as film growth orientation, lattice strain, or R ion size. For example, when (101) orientation orthorhombic HoMnO_3 film grown on Nb-doped SrTiO_3 (111) substrates,²¹ no second magnetic transition of Mn^{3+} is observed, while in the c-axis orientation orthorhombic HoMnO_3 film grown on Nb-doped SrTiO_3 (001),¹⁸ a second magnetic transition shows up. Moreover, when b-axis orientation orthorhombic HoMnO_3 and LuMnO_3 films grown on LaAlO_3 (110) substrates,¹⁹ a second magnetic transition in HoMnO_3 film only appears along c-axis, while the second magnetic transition in the LuMnO_3 film appears along a-, b-, and c-axes. In addition, the second magnetic transition is also anisotropic with a transition temperature of 27 K along the a- and c-axes, and a transition temperature of 35 K along the b-axis. In our case, as described above, the magnetic transition at 27 K only appears along c-axis, not in the ab plane, which is very different from the above orthorhombic LuMnO_3 film although the Sc^{3+} ion size is close to Lu^{3+} ion size, while our case is very similar to the above orthorhombic HoMnO_3 film. This indicates that the second magnetic transition is more prone to substrate-induced lattice strain. To further confirm lattice strain effect, we measured the magnetic properties of thick ScMnO_3 film with thickness of 150 nm, as shown in Figures 4(c) and 4(d). It can be seen in zero-field cooling M-T curve at 1 kOe that antiferromagnetic ordering temperature is still around 47 K; however, the second magnetic transition temperature increases to 36 K, which also only appears along c-axis, not in ab plane, and also is suppressed under a high magnetic field of 10 kOe. This indicates that the second magnetic transition temperature changes with film thickness, suggesting that it is closely related with lattice strain effect. In addition, the second magnetic transition along c-axis is suppressed under a magnetic field of 10 kOe, which is generally thought to be connected with magnetism-induced ferroelectric polarization along c-axis. This is indeed observed in c-axis oriented orthorhombic HoMnO_3 films where the ferroelectric polarization was probed by P - E hysteresis measurements along c-axis at a second magnetic transition temperature near 35 K.²⁰ It was also reported experimentally⁹ that, in orthorhombic HoMnO_3 single crystal, the direction of electric polarization is not along the crystallographic a-axis, as predicted, but along the c-axis, where polarization starts to appear below the lock-in temperature (T_L , the magnetic propagation vector remains locked at a constant value below this temperature), which cannot be detected from normal magnetic measurement. From the analysis above, the second magnetic transition temperature

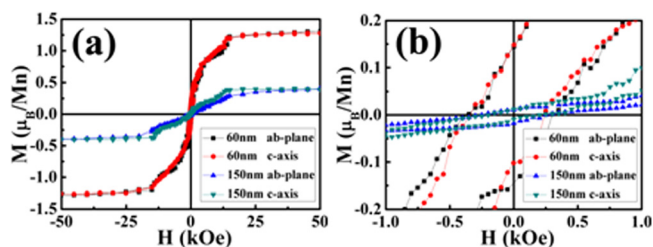


FIG. 5. (a) The magnetic field dependent magnetization of 60 nm and 150 nm ScMnO_3 films along c-axis and in ab plane at 10 K. Figure 5(b) shows an enlarged low field region of the curves in Figure 5(a).

seems to be closely related to the so-called lock-in temperature in orthorhombic RMnO_3 .

Figure 5(a) shows the magnetic-field dependent magnetization of 60 nm and 150 nm ScMnO_3 films along c axis and in ab-plane at 10 K. The obvious ferromagnetic hysteresis from both directions for each film is observed with coercivity of 250 Oe and 200 Oe for 60 nm and 150 nm films, respectively, as shown in Figure 5(b). It is noticed that the saturation magnetization for 60 nm film is about 3 times higher than that for 150 nm film. Similar phenomena were also reported in TbMnO_3 film where saturation magnetization increases with film thickness decreasing. These phenomena verify that low temperature ferromagnetism exists in our films. As introduced above, self-assembly nano-scale crystallographic domain structure can induce ferromagnetism in multiferroic RMnO_3 films.^{22–24} The plane-view TEM measurement of 60 nm film was conducted, and two typical bright field TEM images are shown in Figures 6(a) and 6(b). Self-assembly nano-scale domains are naturally formed in

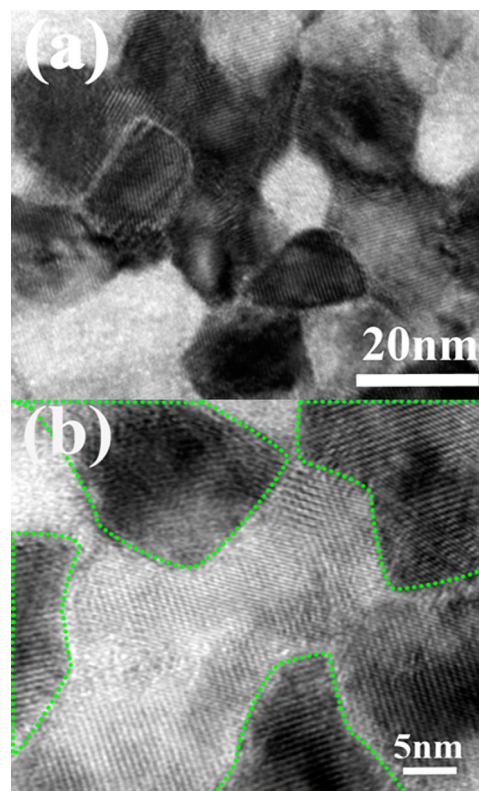


FIG. 6. (a) The bright field plane-view TEM image of 60 nm ScMnO_3 film. Figure 6(b) shows the high resolution TEM image of the same patch.

our film as shown in Figure 6(a) with mean domain size of about 20 nm. These domains are perpendicular to each other, which is very similar to twin-like domain structure in orthorhombic GdMnO_3 and TbMnO_3 films.^{22,23} However, due to small grain size, it is very difficult to obtain a high quality electron diffraction pattern in our case. Domain boundary can be clearly observed in the high resolution TEM image in Figure 6(b). So, we believe that low-temperature ferromagnetism in our films originates from self-assembly nano-scale domain structure. Similar to TbMnO_3 films,²³ enhanced saturation magnetization in 60 nm film is possibly due to formation of high density domain walls in thin film than in thick film. This is also evidenced by higher coercivity in 60 nm film than 150 nm film.

In summary, perovskite orthorhombic ScMnO_3 thin film was fabricated using LaAlO_3 (001) substrate. Investigations on magnetic properties and comparison with those of orthorhombic HoMnO_3 and LuMnO_3 systems clearly show that, besides the normal antiferromagnetic ordering around 47 K, an anomalous second magnetic transition of Mn^{3+} around 27 K for 60 nm and 36 K for 150 nm along the c-axis is caused by substrate induced strain and also closely related to lock-in transition. Obvious ferromagnetism is observed at 10 K with enhanced saturation magnetization in 60 nm film than 150 nm film. This is induced by nano-scaled twin like domain structure of ScMnO_3 films. The detailed magnetic structure will be investigated by the neutron diffraction experiment in the future; in addition, ferroelectric polarization and dielectric constant study will also be carried out to explore larger magneto-electric couple through the control of nano-scale crystallographic domain structure and lattice strain in the future.

This work was supported by the National Nature Science Foundation of China under Projects 51331006 and 51271177.

¹K. F. Wang, J. M. Liu, and Z. F. Ren, *Adv. Phys.* **58**, 321 (2009).

²B. Lorenz, *ISRN Condens. Matter. Phys.* **2013**, 497073 (2013).

- ³Th. Lottermoser, Th. Lonkai, U. Amann, D. Hohlwein, J. Ihringer, and M. Fiebig, *Nature* **430**, 541 (2004).
- ⁴B. Lorenz, A. P. Litvinchuk, M. M. Gospodinov, and C. W. Chu, *Phys. Rev. Lett.* **92**, 087204 (2004).
- ⁵Z. J. Huang, Y. Cao, Y. Y. Sun, Y. Y. Xue, and C. W. Chu, *Phys. Rev. B* **56**, 2623 (1997).
- ⁶I. A. Sergienko, C. Sen, and E. Dagotto, *Phys. Rev. Lett.* **97**, 227204 (2006).
- ⁷S. Picozzi, K. Yamauchi, B. Sanyal, I. A. Sergienko, and E. Dagotto, *Phys. Rev. Lett.* **99**, 227201 (2007).
- ⁸J. S. Zhou and J. B. Goodenough, *Phys. Rev. Lett.* **96**, 247202 (2006).
- ⁹N. Lee, Y. J. Choi, M. Ramazanoglu, W. Ratcliff, II, V. Kiryukhin, and S.-W. Cheong, *Phys. Rev. B* **84**, 020101 (2011).
- ¹⁰J. S. Zhou, J. B. Goodenough, J. M. Gallardo-Amores, E. Morán, M. A. Alario-Franco, and R. Caudillo, *Phys. Rev. B* **74**, 014422 (2006).
- ¹¹K. Uusi-Esko, J. Malm, N. Imamura, H. Yamauchi, and M. Karppinen, *Mater. Chem. Phys.* **112**, 1029 (2008).
- ¹²M. Tachibana, T. Shimoyama, H. Kawaji, T. Atake, and E. Takayama-Muromachi, *Phys. Rev. B* **75**, 144425 (2007).
- ¹³P. Gao, H. Y. Chen, T. A. Tyson, Z. X. Liu, J. M. Bai, L. P. Wang, Y. J. Choi, and S.-W. Cheong, *Appl. Phys. Lett.* **97**, 262905 (2010).
- ¹⁴H. W. Brinks, H. Fjellvåg, and A. Kjekshus, *J. Solid State Chem.* **129**, 334 (1997).
- ¹⁵H. Y. Chen, T. Yu, P. Gao, J. M. Bai, J. Tao, T. A. Tyson, L. P. Wang, and R. Lalancette, *Inorg. Chem.* **52**, 9692 (2013).
- ¹⁶A. A. Belik and W. Yi, *J. Phys.: Condens. Matter* **26**, 163201 (2014).
- ¹⁷T. Yu, T. A. Tyson, P. Gao, T. Wu, X. Hong, S. Ghose, and Y.-S. Chen, *Phys. Rev. B* **90**, 174106 (2014).
- ¹⁸T. H. Lin, H. C. Shih, C. C. Hsieh, C. W. Luo, J.-Y. Lin, J. L. Her, H. D. Yang, C.-H. Hsu, K. H. Wu, T. M. Uen, and J. Y. Juang, *J. Phys.: Condens. Matter* **21**, 026013 (2009).
- ¹⁹T. Y. Tsai, T. H. Lin, S. Slowry, C. W. Luo, K. H. Wu, J.-Y. Lin, T. M. Uen, and J. Y. Juang, *J. Phys.: Conf. Ser.* **200**, 012210 (2010).
- ²⁰T. H. Lin, C. C. Hsieh, C. W. Luo, J.-Y. Lin, C. P. Sun, H. D. Yang, C.-H. Hsu, Y. H. Chu, K. H. Wu, T. M. Uen, and J. Y. Juang, *J. Appl. Phys.* **106**, 103923 (2009).
- ²¹S.-H. Lee, M.-H. Jung, C.-H. Yang, T. Y. Koo, and Y. H. Jeong, *J. Phys.: Conf. Ser.* **200**, 012103 (2010).
- ²²X. Li, C. L. Lu, J. Y. Dai, S. Dong, Y. Chen, N. Hu, G. H. Wu, M. F. Liu, Z. B. Yan, and J. M. Liu, *Sci. Rep.* **4**, 7019 (2014).
- ²³S. Farokhipoor, C. Magén, S. Venkatesan, J. Íñiguez, C. J. M. Daumont, D. Rubi, E. Snoeck, M. Mostovoy, C. de Graaf, A. Müller, M. Döblinger, C. Scheu, and B. Noheda, *Nature* **515**, 379 (2014).
- ²⁴S. Venkatesan, C. Daumont, B. J. Kooi, B. Noheda, and J. Th. M. De Hosson, *Phys. Rev. B* **80**, 214111 (2009).